

Temperature-Dependent Exchange Splitting of a Surface State on a Local-Moment Magnet: Tb(0001)

M. Bode, M. Getzlaff, A. Kubetzka, R. Pascal, O. Pietzsch, and R. Wiesendanger
*Institute of Applied Physics and Microstructure Research Center, University of Hamburg,
Jungiusstrasse 11, D-20355 Hamburg, Germany*

(Received 26 May 1999)

We have investigated the temperature-dependent binding energies of the exchange-split Tb(0001) surface state by means of scanning tunneling spectroscopy. At $T = 16$ K the majority and minority part of the surface state exhibit a binding energy of -135 ± 8 meV and $+430 \pm 15$ meV, respectively. Both peak positions shift with increasing temperature and continuously decrease the exchange splitting down to 200 meV at 260 K, i.e., 30 K above the bulk Néel temperature T_{NB} . This result is explained in terms of a decrease of helical short-range spin order with increasing temperature above T_{NB} .

PACS numbers: 73.20.At, 75.30.Pd, 75.70.Ak

In the past the effort to improve our understanding of finite temperature magnetic properties has mainly concentrated on itinerant ferromagnets like Fe, Co, and Ni. The theoretical starting point was the one-electron finite temperature band theory, which we know under the name “Stoner theory” [1,2]. Within this theory, the characteristic parameter is the exchange splitting Δ_{ex} , defined as the energetic difference between majority and minority spin bands. According to this theory Δ_{ex} decreases with increasing temperature until majority and minority spin bands merge at the Curie temperature T_C . Simultaneously, the magnetic moments disappear. Stoner’s theoretical approach was dedicated to quasifree electrons, a condition which is obviously not fulfilled by the narrow energy d bands that are responsible for magnetism in the itinerant magnets. Instead, strong correlation effects have to be considered which are included in the framework of the “local-band theory” by local moments that remain at an almost constant amplitude but exhibit transverse fluctuations [3]. In the framework of the local-band theory short-range spin order may persist even above T_C although *per definitionem* long-range spin order is lost at the ferromagnetic-paramagnetic phase transition. Indeed, transverse spin fluctuations have recently been observed on Ni(110) [4]. Nowadays it is widely accepted that the question whether or not the exchange splitting collapses in itinerant ferromagnets at or above T_C substantially depends on the degree of localization of the considered electron bands which has to be compared with the size of regions that exhibit short-range spin order. As a consequence, Δ_{ex} may exhibit a striking k dependence [5,6].

In contrast, for magnetic materials with localized magnetic moments only very few data are available. Experimental effort to gain a reliable data basis on the temperature-dependent exchange splitting has concentrated on the (0001) surfaces of the rare-earth (RE) metals Gd [7–13] and Tb [14]. While Gd is ferromagnetic (FM) below its bulk Curie temperature $T_{CB} = 293$ K, the bulk material of Tb exhibits two magnetic phases: it is (i) FM

below $T_{CB} = 220$ K and (ii) antiferromagnetic (AFM) with a helical magnetic structure between T_{CB} and the bulk Néel temperature $T_{NB} = 228$ K. In the case of Gd(0001) it has been consistently described by experimentalists that the bulk majority and minority spin bands, occupied [7,8] as well as empty [9,10], merge at the bulk Curie temperature $T_{CB} = 293$ K. This Stoner-like behavior might be caused by their itinerant character. However, contradictory experimental results have been published concerning the exchange splitting of the RE(0001) surface state. This surface state exhibits a d_{z^2} -like symmetry, is strongly localized, and was made responsible for so-called extraordinary surface magnetic properties [15–17]. While it was claimed for Gd(0001) in a spin-polarized photoelectron spectroscopy (PES) study that the occupied majority part of the surface state exhibits no energetic shift with increasing temperature but instead loses spin polarization (so-called spin-mixing behavior) [8], another combined (inverse)PES study came to the result that occupied majority and empty minority spin bands merge together [11]. Surprisingly enough, the same group applying the same experimental techniques reported on spin-mixing behavior for the surface state of Tb(0001) [14], a material which exhibits electronic properties being very similar to Gd(0001) [18,19]. A recent scanning tunneling spectroscopy (STS) study [12,13] revealed that the temperature-dependent exchange splitting Δ_{ex} of Gd(0001) can neither be described by a pure spin mixing nor by a pure Stoner-like behavior. Instead, Δ_{ex} of Gd(0001) decreases up to $T_{CB} = 293$ K but then remains constant within our measurement accuracy up to $T = 360$ K.

In this Letter, we present STS data on the temperature-dependent behavior of the exchange-split surface state of Tb(0001). In contrast to Gd(0001) we found that the Tb(0001) exchange splitting does not remain constant above T_{CB} and T_{NB} but continues to decrease with increasing temperature up to about 260 K, i.e., 40 K above T_{CB} . We will show that—in combination with the localized nature of the RE surface state—the question whether Δ_{ex}

changes above T_{NB} or T_{CB} is related to the type of short-range spin order that persists, i.e., helical AFM or FM.

The experiments have been performed in three different UHV systems each equipped with a scanning tunneling microscope (STM) for operation either at low ($T = 16$ K), variable ($20 \text{ K} \leq T \leq 380$ K), or at room temperature ($T = 293$ K), respectively. The base pressure was always below $p = 1 \times 10^{-10}$ mbar. Typically, Tb films of 100 ± 10 ML (monolayer) thickness were grown on a W(110) substrate at a rate of 3 ML/min ($p < 6 \times 10^{-10}$ mbar) and subsequently annealed to 900 K for 10 min. Spectroscopical STM data are gained by measuring the derivative of the tunneling current I with respect to the applied sample bias voltage U , the so-called dI/dU signal, by means of a lock-in technique. All tunneling spectra presented below were acquired by scanning the sample at a particular temperature and measuring one dI/dU spectrum at every pixel. By varying the stabilization gap voltage between $-0.8 \leq U \leq 0.8$ V and the tunneling current between $0.1 \leq I \leq 10$ nA we found the results do not depend on the tunneling stabilization parameters.

Figure 1(a) shows a single tunneling dI/dU spectrum measured at a sample temperature $T = 16$ K above a 100 ± 10 ML thick Tb(0001) film epitaxially grown on a W(110) substrate. The topography of such a film as measured in a constant-current STM image is shown in the inset of Fig. 1(a). The sample topography is dominated

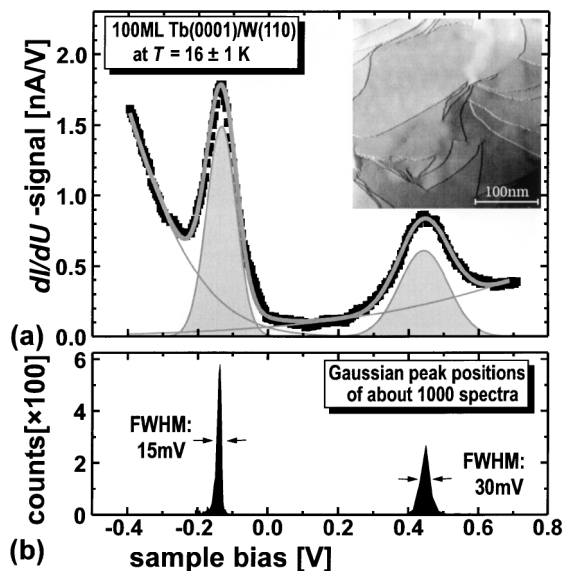


FIG. 1. (a) A single tunneling dI/dU spectrum measured at $T = 16 \pm 1$ K above a 100 ML thick Tb(0001) film grown on W(110) (■). The inset shows the typical sample topography ($I = 0.4$ nA, $U = -0.4$ V). The dI/dU spectrum can be fitted by the sum of four Gaussian functions (thick grey line). Two Gaussians represent the empty and occupied parts of the Tb(0001) surface state while the others represent the background. (b) Histogram of peak positions as determined by a Gaussian-fit procedure individually applied to the surface state peaks of about 1000 tunneling spectra.

by atomically flat terraces and monatomic steps. The Tb(0001) surface exhibits numerous double screw dislocations. These films gave a sharp (1×1) LEED pattern. The particular dI/dU spectrum of Fig. 1(a) exhibits two peaks, a rather broad one at positive and a narrower one at negative sample bias. These peaks represent the empty and occupied parts of the Tb(0001) surface state, respectively. This identification is supported by the fact that the peak position of the majority part in our tunneling spectra is in good accordance with photoemission data obtained at low temperature [14]. As characteristic for a surface state the adsorption of hydrogen quenches both peaks (not shown here). A similar behavior has been observed for Gd(0001) [20,21]. We have fitted the spectrum of Fig. 1(a) by the sum of four Gaussian functions. Two Gaussians close to the Fermi level E_F , i.e., at $U = 0$ V, represent the empty and occupied parts of the Tb(0001) surface state. For this particular spectrum we find peak positions of $U = +434$ mV and $U = -142$ mV, respectively. Furthermore, two broad Gaussian functions with peaks far outside of the energy range of interest simulate the background of the spectrum that rises on both sides of the Fermi level. Comparison between experimental data and the fit reveals an excellent overall agreement. By applying this procedure to each spectrum measured within the scan above flat terraces and adding the derived peak positions to a histogram [Fig. 1(b)] we receive two sharp peaks at $U = +430 \pm 15$ and at $U = -135 \pm 8$ mV.

Figure 2 shows typical tunneling spectra of Tb(0001) (black line) and histograms of the peak positions (grey)

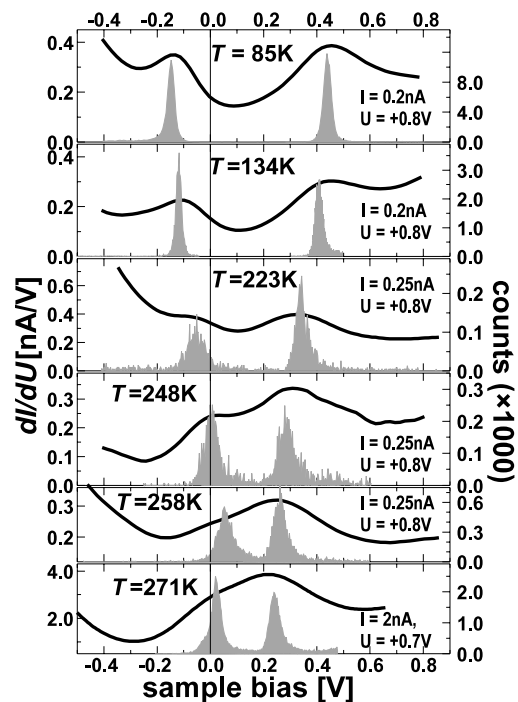


FIG. 2. Tunneling spectra (left scale) and histograms of the surface state peak positions (right scale) of Tb(0001) measured at various temperatures.

measured at six selected temperatures between $T = 85$ and $T = 271$ K, thereby covering a temperature range that includes all three possible phase transitions, i.e., bulk FM \rightarrow bulk AFM, bulk AFM \rightarrow bulk paramagnetic (PM), and surface FM \rightarrow surface PM. At $T = 85$ K the dI/dU spectrum exhibits two distinct maxima at sample biases of $U = 440 \pm 20$ and $U = -150 \pm 20$ mV, again representing the empty and occupied parts of the exchange-split Tb(0001) surface state, respectively. By increasing the sample temperature both peaks shift towards E_F thereby decreasing the exchange splitting Δ_{ex} . Just above T_{CB} ($T = 223$ K) the occupied part of the surface state has already approached the Fermi level very closely ($U = -50 \pm 34$ mV). In contrast to our earlier experiments on Gd(0001), we found that this trend continues for Tb(0001) even above its bulk magnetic phase transition temperatures $T_{\text{CB}} = 220$ and $T_{\text{NB}} = 228$ K. At $T = 248$ K the former occupied part of the surface state is energetically located at the Fermi level ($U = 10 \pm 30$ mV). When further increasing the temperature ($T = 258$ K and $T = 271$) the maximum in the dI/dU spectra crosses E_F . As a result the surface state which was clearly occupied at low temperature ($T = 85$ K) becomes partially empty above $T = 250$ K.

In Fig. 3 we have summarized the temperature-dependent peak positions of the “filled” and empty parts of the Tb(0001) surface state. Furthermore, for comparison we have included data obtained on Gd(0001) [12,13]. We used different temperature scales for Gd (top axis) and Tb (bottom axis) such that the data can be compared in terms of a reduced temperature T/T_{CB} . While both parts of the surface state shift only slightly by about 100 meV towards E_F between $T = 16$ K and T_{CB} , a more rapid shift towards E_F is observed when increasing the temperature above T_{CB} , i.e., within the narrow temperature

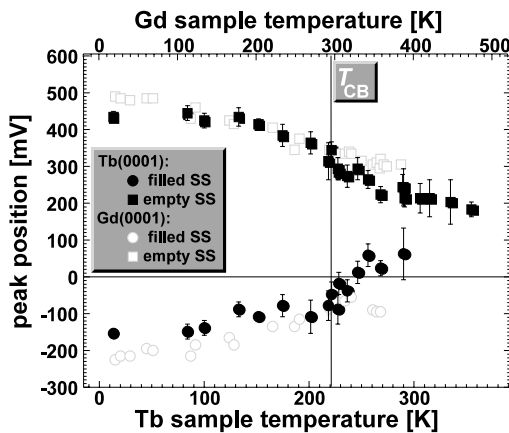


FIG. 3. Plot of the peak positions of the Tb(0001) surface state versus the sample temperature (bottom axis). While the empty part (■) of the surface state shifts from +440 mV at 85 K down to +180 mV at 360 K the occupied part (●) moves from -150 mV at 85 K to about +40 mV at 270 K, thereby crossing the Fermi level at about 250 K. For comparison we have included data obtained on Gd(0001) (top axis).

range $T_{\text{CB}} < T < 265 \pm 5$ K both parts of the surface state exhibit a further shift of about 120 meV. This leads to the fact that the maximum of the occupied part of the surface state crosses E_F at about 250 K, thereby becoming partially unoccupied. Above about 265 K the peak positions remain constant within the error bar.

If we compare the temperature-dependent surface electronic behavior of Tb(0001) to that of Gd(0001), it is the most apparent qualitative difference that the second temperature regime—being characterized by a rapid shift of both parts of the surface state towards E_F above T_{CB} —does not exist for Gd(0001). Instead, the first temperature regime is directly followed by the third, i.e., by increasing the Gd(0001) sample temperature above T_{CB} we found peak positions that remain constant within our measurement accuracy. The difference becomes even more obvious when we compare the surface state exchange splitting Δ_{ex} of Gd(0001) and Tb(0001) as shown in Fig. 4. Close to the ground state Tb exhibits a Δ_{ex} of 600 meV while it amounts to 700 meV for Gd(0001), thereby reflecting their ratio of the local $4f$ moment of $7\mu_B$ in the case of Gd and $6\mu_B$ in the case of Tb. Δ_{ex} decreases with increasing temperature down to about 400 meV at T_{CB} for both, Gd and Tb. However, increasing T above T_{CB} leads to a further reduction of Δ_{ex} for Tb(0001), while it remains constant for Gd(0001). Only for $T > 260$ K the data obtained on Tb(0001) suggest a constant value of Δ_{ex} .

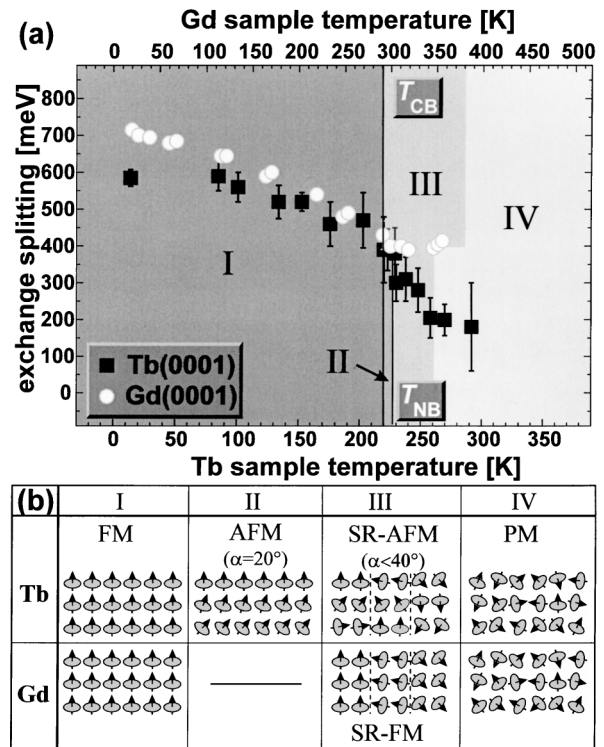


FIG. 4. (a) Temperature-dependent surface exchange splitting of the Tb(0001) (■) and Gd(0001) (○) surface states. (b) Schematic spin structures of Tb and Gd: (I) ferromagnetic (FM), (II) anti-ferromagnetic (AFM), (III) short-range AFM and short-range FM, and (IV) paramagnetic (PM).

This striking difference between the temperature-dependent surface electronic properties of Tb(0001) and Gd(0001) is strongly related to the question which type of short-range spin order persists above T_{NB} and T_{CB} , respectively, i.e., helical AFM or FM order. In this context it is important that the d_{z^2} -like surface state which exists on RE(0001) surfaces is strongly localized at each surface atom with a small overlap to nearest neighbors (NN) underneath [17]. Therefore, the amount of exchange splitting is governed by the degree of collinearity between the $4f$ moments of a particular atom and its NN. Below T_{CB} and T_{NB} the $4f$ moments exhibit long-range FM and helical AFM order, respectively, as schematically presented in columns I and II of Fig. 4(b). Gd is the only magnetic RE metal that exhibits no spiral magnetic phase. Instead, strong evidence exists that short-range FM order [cf. column III of Fig. 4(b)] persists “up to at least 340 K,” possibly up to 400 K [22]. A recent spin-polarized photoelectron study revealed that the Gd(0001) surface exhibits short-range (>20 Å) FM spin order up to about 380 K, too [23]. In contrast to Gd, most other RE metals exhibit short-range helical spin order in the PM state. In the case of bulk Tb—as well as in other RE metals like Dy and Ho—“AFM order persists ≈ 40 K above T_{NB} ” [24]. This value corresponds to the temperature range for which we found a rapidly decreasing exchange splitting Δ_{ex} , i.e., $T_{NB} \leq T \leq 260$ K [cf. Fig. 4(a)]. While the helical turn angle ω of Tb amounts to 20° between adjacent basal planes within the AFM phase, it rises up to 40° between T_{NB} and 260 K [24]. With this in mind it is straightforward to explain the striking difference between Tb(0001) and Gd(0001) in regime III of Fig. 4(a): The exchange splitting Δ_{ex} of the Gd(0001) surface state remains constant above T_{CB} up to at least 360 K (probably up to 380 K) because it remains ferromagnetically ordered on the relevant length scale, i.e., several lattice constants. In contrast, for Tb the angle ω increases from 20° at 228 K up to 40° at 260 K, resulting in a more and more noncollinear arrangement of the $4f$ moments with increasing temperature. Finally, in the PM regime (IV) any spin order is lost. Nevertheless, due to the high spatial localization of the surface state which still interacts with the atomic $4f$ magnetic moments a small local Δ_{ex} is maintained.

It remains, however, the question whether Tb(0001) exhibits an enhanced surface T_C (T_{CS}) as claimed by Rau *et al.* on the basis of electron capture spectroscopy (ECS) [16]. The results of this study show that the electron spin polarization remains nonzero up to 248 K, but shows a striking nonmonotonic behavior, i.e., it increases with increasing temperature above 240 K and peaks at ≈ 245 K. In this context it is worthwhile, however, to mention that ECS favors electronic states that are energetically located close to E_F with the momentum vector \vec{k} roughly along the surface normal [25]. Furthermore, the ECS experiments have not been performed in remanence but in an external magnetic field between 25 and 600 Oe.

Therefore, regions that exhibit short-range order are forced into a parallel alignment above T_{CB} . At about $T = 250$ K the “occupied” part of the Tb(0001) surface state which is localized around the $\bar{\Gamma}$ point of the surface Brillouin zone crosses E_F (cf. Fig. 3). As a result both conditions for an enhanced ECS signal are fulfilled and a peak of the measured spin polarization is observed.

In summary, we have investigated the temperature-dependent surface electronic structure of Tb(0001) by means of STS and compared it to data previously obtained on Gd(0001). Our results show that both, the filled as well as the empty part of the Tb(0001) surface state, shift towards E_F with increasing temperature thereby reducing Δ_{ex} , which exhibits 600 meV in the ground state, down to 400 meV at T_{CB} . In contrast to Gd, Δ_{ex} of Tb further decreases when increasing T above T_{CB} and T_{NB} up to about 260 K. We have shown that the behavior of both metals can be understood by different types of short-range spin order that persist above the highest transition temperature of both materials.

Financial support from the Deutsche Forschungsgemeinschaft is gratefully acknowledged.

-
- [1] E. C. Stoner, Proc. R. Soc. London A **154**, 656 (1936).
 - [2] E. P. Wohlfarth, Rev. Mod. Phys. **25**, 211 (1953).
 - [3] V. Korenman, J. L. Murray, and R. E. Prange, Phys. Rev. B **16**, 4023 (1977); **16**, 4048 (1977); **16**, 4058 (1977).
 - [4] A. Kakizaki *et al.*, Phys. Rev. Lett. **72**, 2781 (1994).
 - [5] J. Kirschner *et al.*, Phys. Rev. Lett. **53**, 612 (1984).
 - [6] P. Aebi *et al.*, Phys. Rev. Lett. **76**, 1150 (1996).
 - [7] B. Kim *et al.*, Phys. Rev. Lett. **68**, 1931 (1992).
 - [8] D. Li *et al.*, Phys. Rev. B **51**, 13 895 (1995).
 - [9] A. V. Fedorov, K. Starke, and G. Kaindl, Phys. Rev. B **50**, 2739 (1994).
 - [10] M. Donath, B. Gubanka, and F. Passek, Phys. Rev. Lett. **77**, 5138 (1996).
 - [11] E. Weschke *et al.*, Phys. Rev. Lett. **77**, 3415 (1996).
 - [12] M. Bode *et al.*, Appl. Phys. A **66**, S121 (1998).
 - [13] M. Getzlaff *et al.*, J. Magn. Magn. Mater. **184**, 155 (1998).
 - [14] F. Hübingner *et al.*, J. Electron. Spectrosc. Relat. Phenom. **76**, 535 (1995).
 - [15] H. Tang *et al.*, Phys. Rev. Lett. **71**, 444 (1993).
 - [16] C. Rau, C. Jin, and M. Robert, Phys. Lett. A **138**, 334 (1989).
 - [17] R. Wu *et al.*, Phys. Rev. B **44**, 9400 (1991).
 - [18] S. C. Wu *et al.*, Phys. Rev. B **44**, 13 720 (1991).
 - [19] R. Ahuja *et al.*, Phys. Rev. B **50**, 5147 (1994).
 - [20] R. Pascal *et al.*, Appl. Phys. A **65**, 603 (1997).
 - [21] M. Getzlaff, M. Bode, and R. Wiesendanger, Surf. Sci. **410**, 189 (1998).
 - [22] H. E. Nigh, S. Legvold, and F. H. Spedding, Phys. Rev. **132**, 1092 (1963).
 - [23] E. D. Tober *et al.*, Phys. Rev. Lett. **81**, 2360 (1998).
 - [24] R. D. Greenough *et al.*, J. Magn. Magn. Mater. **29**, 67 (1982).
 - [25] H. Schröder, Nucl. Instrum. Methods Phys. Res. **194**, 381 (1982).